Clays and Clay Minerals, Vol. 38, No. 4, 337–342, 1990.

MOLECULAR-SCALE IMAGING OF CLAY MINERAL SURFACES WITH THE ATOMIC FORCE MICROSCOPE

H. HARTMAN

Department of Electrical Engineering and Computer Science, University of California
Berkeley, California 94720

GARRISON SPOSITO AND ANDREW YANG

Department of Soil Science, University of California, Berkeley, California 94720

S. MANNE, S. A. C. GOULD, AND P. K. HANSMA

Department of Physics, University of California, Santa Barbara, California 93106

Abstract—Specimen samples of Crook County montmorillonite and Silver Hill illite, purified and prepared in the Na-form, were imaged under 80% relative humidity using an atomic force microscope. The direct images showed clearly the hexagonal array of hexagonal rings of oxygen ions expected for the basal planes of 2:1 phyllosilicates. Fourier transformation of the digital information obtained by the microscope scanning tip led to an estimate of 5.1 ± 0.3 Å for the nearest-neighbor separation, in agreement with the ideal nearest-neighbor spacing of 5.4 Å for hexagonal rings as derived from X-ray powder diffraction data. The atomic force microscope should prove to be a useful tool for the molecular-scale resolution of clay mineral surfaces that contain adsorbed macromolecules.

Key Words—Atomic force microscopy, Illite, Montmorillonite, Oxygen distances, Surface.

INTRODUCTION

The atomic force microscope (AFM) is a recent innovation in instrumentation that provides topographic images, at the Ångstrom scale, of the surfaces of solid materials. Since the invention of the AFM by Binnig *et al.* (1986), a variety of scanned-probe microscopes based loosely on the principle of the AFM has been developed (Wickramasinghe, 1989). The AFM described by Drake *et al.* (1989) and used in the present study operates in the contact mode, in which the scanning tip gently touches the sample surface. This type of AFM has been utilized to investigate the atomic-scale structure of albite, graphite, boron nitride, and molybdenum bisulfide (Albrecht and Quate, 1988; Hochella *et al.*, 1990); of polymer chains of alanine and the real-time polymerization of fibrin monomers (Drake *et al.*, 1989); and of blood cells, bacteria, and integrated circuit chips (Gould *et al.*, 1990). Sample preparation for AFM examination of mineral surfaces is relatively straightforward, and surfaces can be imaged under water or aqueous solutions. Because the typical scan time for a surface patch is on the order of seconds, direct imaging of localized surface phenomena in real time is possible.

In this paper, we report the first atomic force microscope images of clay mineral surfaces. Cleaned surfaces of montmorillonite and illite were imaged in air under relative humidities near 80%, corresponding to a few molecular layers of adsorbed water. The objective of the study was to provide molecular-scale images of the clay mineral surfaces as the basis for future investigations of clay-polymer reactions in aqueous media.

EXPERIMENTAL

Sodium-form clay minerals

The clay minerals investigated were a montmorillonite from Crook County, Wyoming, and Silver Hill illite from Jefferson Canyon, Montana. Samples of both minerals were obtained from the Source Clays Repository of The Clay Minerals Society. With Na^+ as the exchangeable cation, the unit-cell formulae of these two dioctahedral 2:1 clay minerals are (Hower and Mowatt, 1966; Weaver and Pollard, 1973):

$$Na_{0.62}(Si_{7.8}Al_{0.2})[Al_{3.28}Fe(III)_{0.30}Fe(II)_{0.04}Mg_{0.38}]O_{20}(OH)_4$$

and

$$Na_{0.12}K_{1.35}(Si_{7.32}Al_{0.68})[Al_{2.76}Fe(III)_{0.52}Fe(II)_{0.14}Mg_{0.56}]O_{20}(OH)_4,$$

respectively, where parentheses refer to the tetrahedral sheet and brackets to the octahedral sheet. The two minerals differ primarily in layer charge (0.62 vs. 1.47) and cationic substitution pattern, but both exhibit siloxane basal planes having unit-cell dimensions of $a = 5.2$ Å, $b = 9.0$ Å $= \sqrt{3}a$ (Brindley and Brown, 1980, pp. 58, 172, 182).

Copyright © 1990, The Clay Minerals Society

https://doi.org/10.1346/CCMN.1990.0380401 Published online by Cambridge University Press

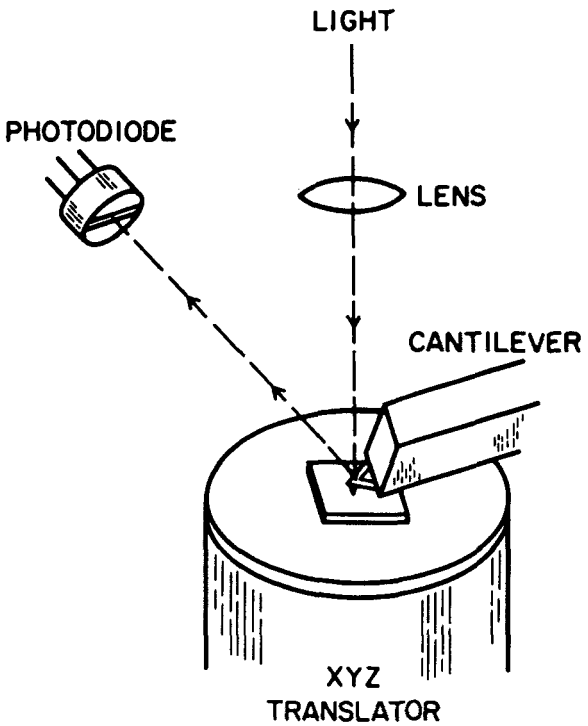


Figure 1. Schematic diagram of the atomic force microscope. Laser light is focused on a cantilever, which reflects it toward a photodiode. The photodiode senses the deflection of the cantilever by sensing the position of the reflected beam. In operation, a feedback loop keeps the position of the reflected beam and hence, force on the sample, constant. This is accomplished by moving the sample up and down with the z-axis of the xyz translator as the sample is scanned underneath it with the x- and y-axes.

The methods by which the clay mineral samples were purified to remove surface coatings of Al hydrous oxides and by which they were prepared in the Na-form were described exhaustively by Sposito *et al.* (1981) for montmorillonite and by Sposito and LeVesque (1985) and Thellier and Sposito (1988) for illite. Briefly, the raw clay sample was fractionated by sedimentation, then washed repeatedly with 1 M $NaClO_4$ at pH 3. The suspension was then treated with 0.05 M $NaClO_4$ at pH 7 until the supernatant solution pH exceeded 6. Details of the washing procedure and data on the composition of the supernatant solutions during washing were given by Thellier and Sposito (1988). The final Na-form product has been shown by X-ray powder diffraction and infrared spectroscopy to be a purified clay mineral having a basal-plane surface free of Al hydroxy material.

The preparation of the clay minerals for microscopic examination involved drying thick suspensions either directly (illite) or first on Mylar film (montmorillonite) on circular (1.08-cm diameter, 0.8-mm thick) stainless steel pedestals placed in a desiccator over P_2O_5 at 22°C. Dried samples that showed no macroscopic evidence of cracking or peeling were selected for examination.

Atomic force microscope

The basic design of the AFM used in this study was from Meyer and Amer (1988) and Alexander *et al.* (1989). A schematic diagram of the AFM is shown in Figure 1. The 10-μm diamond tip scans gently (applied force $\approx$ 0.1 μN in air) over the surface topography of a sample, deflecting in response to molecular features. The tip is attached to a microfabricated triangular cantilever about 100 μm long having a force constant of 0.6 N/m (Albrecht and Quate, 1988). Deflections of the cantilever are detected via changes in intensity differences between reflected laser light beams striking two segments of a split photodiode. The motion of the light beam at the photodiode is amplified about 800-fold as a result of the distance ratio in the optical lever. An effective noise contribution of about 0.2 Å exists in the amplified image.

Coarse movement of the cantilever toward the sample is achieved with two fine screws that are turned by hand and one that is driven with a stepper motor. Once contact is achieved, the sample is scanned with a single-tube XYZ piezoelectric crystal translator having a range of about 0.9 μm. Feedback electronics move the sample surface along the z-axis of the translator so as to keep the reflected light beam position constant while the sample is raster-scanned along the x- and y-axes, with control through the application of appropriate voltages to the piezoelectric crystal. At each (x, y) point, the z-axis extension of the piezoelectric crystal is recorded digitally and represented graphically on a gray scale. A complete scan requires a few seconds.

Sample surfaces can be imaged under water or aqueous solutions by construction of a simple cell comprising an O-ring and plexiglas cover. In the present study, however, the clay mineral samples were imaged in air under a relative humidity near 80%, corresponding to 2–3 molecular layers of adsorbed water (Newman, 1987, p. 257).

RESULTS AND DISCUSSION

Representative AFM images of the basal-plane surfaces of Crook County montmorillonite and Silver Hill illite are shown in Figures 2 and 3, respectively. In each photomicrograph, the field of the image is a square of side 66 Å (4356 Å^2, or about 90 unit cells), and the shading ranging from black to white indicates a depth range of about 5–6 Å. The "braided" appearance of the illite image as opposed to the "kernel" appearance of the montmorillonite image may reflect differences in surface structure related to local differences in crystallinity of the two clay minerals (Bailey, 1984, 496–503; 1988, 497–505). On the other hand, they could be the result of variable structural properties of the scanning tip at the molecular scale (Gould *et al.*, 1989).

https://doi.org/10.1346/CCMN.1990.0380401 Published online by Cambridge University Press

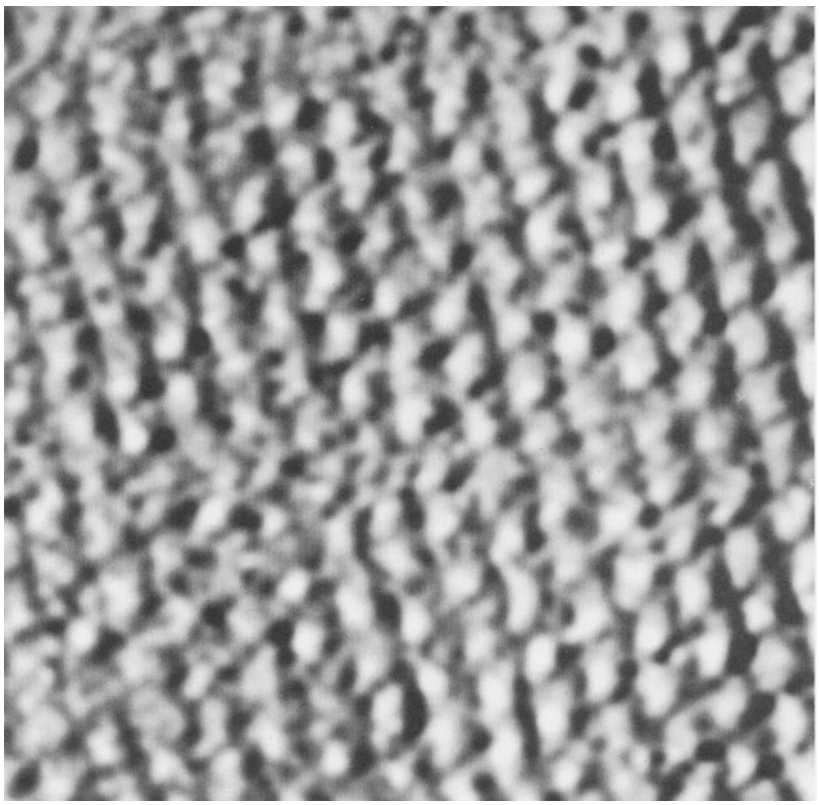


Figure 2. Atomic force microscope image of a 4356 Å² patch of a Na-montmorillonite surface.

The same tip was used to produce both clay mineral images, but the tip shape could not be controlled at the atomic level.

The true surface features revealed by the AFM images are their "clean" appearance, thereby substantiating the efficacy of the clay purification procedures, and the more-or-less regular array of "light" spots. The local ordering of the "light" spots is hexagonal. This fact can be appreciated easily by counting six columns from the right corner along the bottom in either Figure 2 or 3, then counting up either eight (montmorillonite) or seven (illite) "light" spots. In both photographs, one stops at the lower right vertex of a centered hexagon whose base makes an angle of about 20° with the horizontal direction defined by the bottom border of the figure. The transverse center-to-center distance across the hexagons is about 11 Å, as measured with the scale of the photomicrograph.

Figure 4 is a diagram of the ideal hexagonal array of oxygen ions in the siloxane surface of a 2:1 clay mineral (Bailey, 1984, p. 1). The unit cell is shown as a rectangle in dark outline, and a hexagon of oxygen ion hexagons is highlighted in gray tone. Reference to Figure 4 suggests that each of the "light" spots imaged in Figures 2 and 3 is in fact a (hexagonal) ring of oxygen ions, which make a hexagonal array on the basal planes of the two clay minerals. The ideal transverse distance from the center of one ring to another across the hexagon they make is 11 Å, in agreement with what can be seen in Figures 2 and 3. The unit cell shown in Figure 4 includes essentially one ring plus two oxygen ions linking it to neighboring rings. This feature is resolved only as a spot of variable shading in Figures 2 and 3. Thus, resolution below the scale of the unit cell was not achieved.

The nearest-neighbor distance between the "light" spots in Figures 2 and 3 can be estimated reasonably well by calculating a two-dimensional fast-Fourier transform of the spatial information obtained with the scanning tip—the mathematical equivalent of obtaining a diffraction pattern of the surface. The resulting two-dimensional transform plots had a decided hexagonal appearance and led to nearest-neighbor distances of 5.0 ± 0.3 Å for montmorillonite and 5.2 ± 0.3 Å for illite, after careful calibration of the two-dimensional transform plot for an AFM image of the muscovite surface against the known muscovite surface spacing. Given a diameter of 2.8 Å for oxygen ions and 2.6 Å for the cavity in a hexagonal ring (Sposito, 1984, pp. 3, 14), the nearest-neighbor distance ex-

https://doi.org/10.1346/CCMN.1990.0380401 Published online by Cambridge University Press

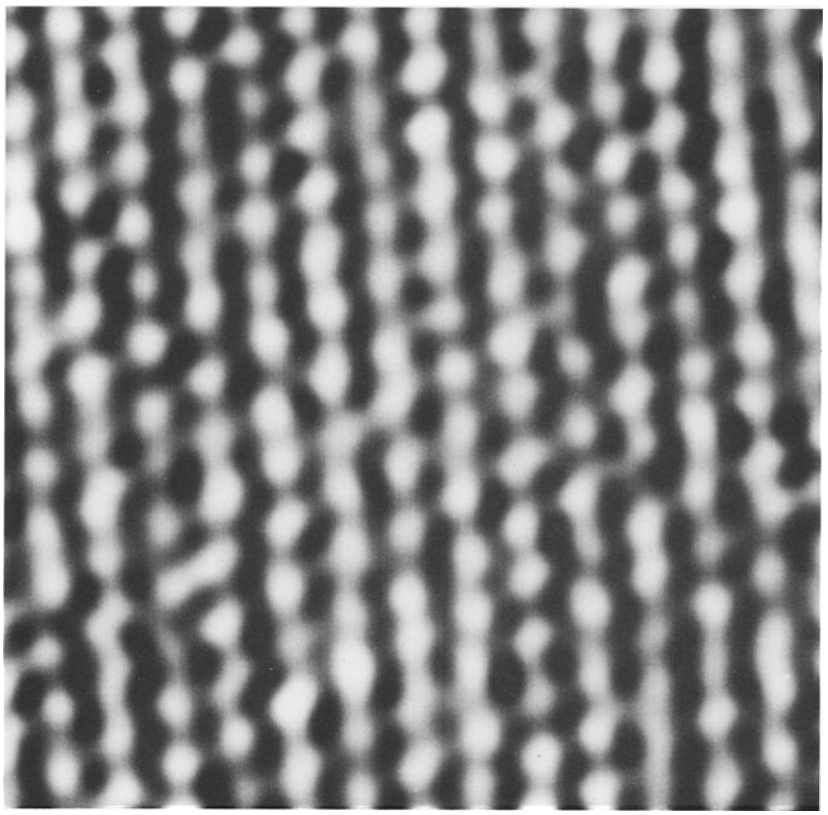


Figure 3. Atomic force microscope image of a 4356 Å^2 patch of a Na-illite surface.

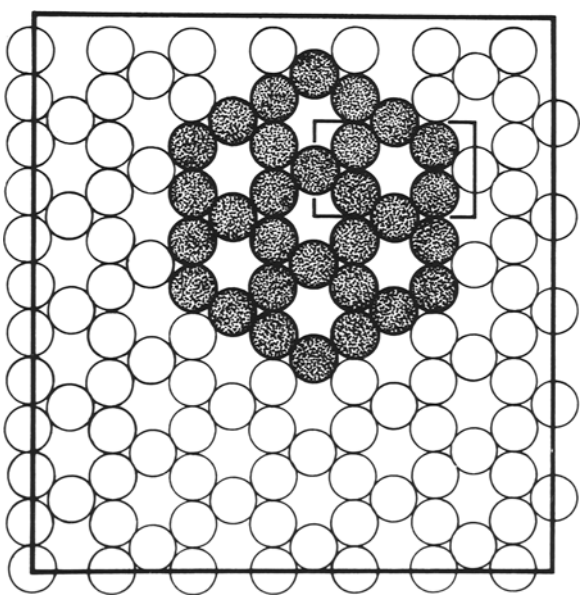


Figure 4. Molecular arrangement of oxygen ions on the basal planes of 2:1 clay minerals. A hexagonal array of (hexagonal) oxygen rings is highlighted, and a unit cell is shown by solid lines.

pected from Figure 4 is 5.4 Å, in agreement with the Fourier transform calculations. This is strong evidence supporting the interpretation of the individual "light" spots as hexagonal rings of oxygen ions.

The digital information obtained from a scan also was resolved into contours representing surfaces of constant height. Contour diagrams for Figures 2 and 3 are shown in Figures 5 and 6. In these diagrams considerable irregularity appears to exist locally within the regular hexagonal array of oxygen rings. Comparison of the hexagons in the sixth columns of the two contour diagrams with those discussed above in Figures 2 and 3 is helpful in appreciating this point.

CONCLUDING REMARKS

The atomic force microscope can be used to image local molecular environments on the basal surfaces of 2:1 clay minerals with a resolution of about 5 Å, i.e., a unit-cell dimension. No unusual desiccation of the sample or ultrahigh vacuum conditions are required, allowing natural clay mineral surfaces to be investigated with little disturbance of their molecular features. Of particular interest is the imaging of reactive polymeric organic and inorganic materials whose molecules

https://doi.org/10.1346/CCMN.1990.0380401 Published online by Cambridge University Press

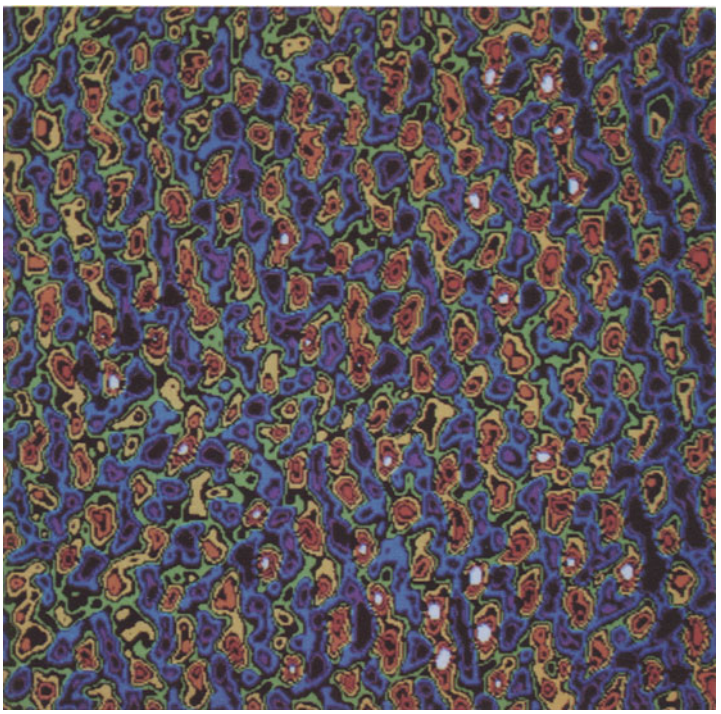


Figure 5. Color contour diagram illustrating the detailed vertical structure of the array of "light" spots in Figure 2.

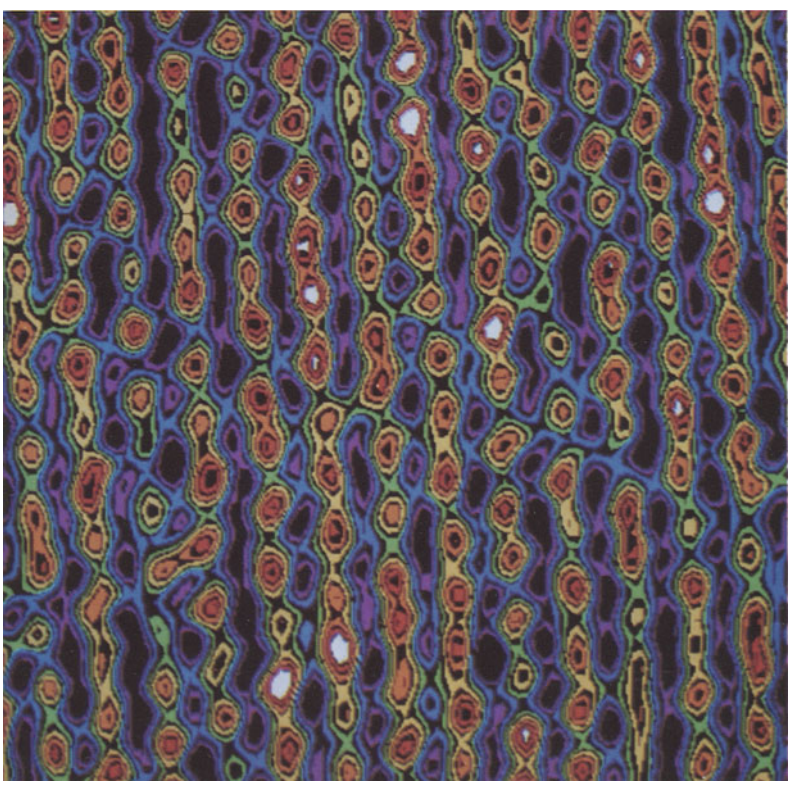


Figure 6. Color contour diagram illustrating the detailed vertical structure of the array of "light" spots in Figure 3.

https://doi.org/10.1346/CCMN.1990.0380401 Published online by Cambridge University Press

cover several unit cells when adsorbed on the basal planes (Theng, 1979). Because of the relatively short time required to execute a scan with the AFM, the imaging of certain kinetic phenomena involving adsorbed macromolecules also may be possible.

ACKNOWLEDGMENTS

We thank V. Elings, J. Massie, J. Gurley, and others at Digital Instruments for donating Nanoscope II electronics and for their assistance in our research; T. R. Albrecht and C. Quate at Stanford University for providing us with the microfabricated cantilevers, which were essential for our research; Greg Kelderman for tip assembly; and Albrecht Weisenhorn for instruction. This project was supported in part by National Science Foundation grant No. DMR86-113486 (S.M., S.A.C.G., P.K.H.) and in part by a grant from the Kearney Foundation of Soil Science (G.S., A.Y.). We are grateful to Terri DeLuca for her excellent typing of the manuscript.

REFERENCES

Albrecht, T. R., and Quate, C. F. (1988) Atomic resolution with the atomic force microscope on conductors and nonconductors: *J. Vac. Sci. Technol.* **A6,** 271–274.

Alexander, S., Hellemans, L., Marti, O., Schneir, J., Elings, V., Hansma, P. K., Longmire, M., and Gurley, J. (1989) An atomic-resolution atomic-force microscope implemented using an optical lever: *J. Appl. Phys.* **65,** 164–167.

Bailey, S. W., ed. (1984) *Micas: Reviews in Mineralogy, Vol. 13:* Mineralogical Society of America, Washington, D.C., 584 pp.

Bailey, S. W., ed. (1988) *Hydrous Phyllosilicates: (Exclusive of micas), Reviews in Mineralogy, Vol. 19:* Mineralogical Society of America, Washington, D.C., 725 pp.

Binnig, G., Quate, C. F., and Gerber, Ch. (1986) Atomic force microscope: *Phys. Rev. Lett.* **56,** 930–933.

Brindley, G. W. and Brown, G. (1980) *Crystal Structures of Clay Minerals and their X-ray Identification:* Mineralogical Society, London, 495 pp.

Drake, B., Prater, C. B., Weisenhorn, A. L., Gould, S. A. C., Albrecht, T. R., Quate, C. F., Cannell, D. S. Hansma, H. G., and Hansma, P. K. (1989) Imaging crystals, polymers, and processes in water with the atomic force microscope: *Science* **243,** 1586–1588.

Gould, S. A. C., Burke, K., and Hansma, P. K. (1989) Simple theory for the atomic-force microscope with a comparison of theoretical and experimental images of graphite: *Phys. Rev.* **B40,** 5363–5366.

Gould, S. A. C., Drake, B., Prater, C. B., Weisenhorn, A. L., Manne, S., Hansma, H. G., Hansma, P. K., Masse, J., Longmire, M., Elings, V., Dixon Northern, B., Mukergee, B., Peterson, C. M., Stoeckenius, W., Albrecht, T. R., and Quate, C. F. (1990) From atoms to integrated-circuit chips, blood cells and bacteria with the atomic force microscope: *J. Vac. Sci. Technol.* **A8,** 369–375.

Hochella, M. F., Eggleston, C. M., Elings, V. B., and Thompson, M. S. (1990) Atomic structure and morphology of the albite (010) surface: An atomic-force microscope and electron diffraction study: *Amer. Mineral.* (in press).

Hower, J. and Mowatt, T. C. (1966) The mineralogy of illites and mixed-layer illite-montmorillonites: *Amer. Mineral.* **51,** 825–854.

Meyer, G. and Amer, N. M. (1988) Erratum: Novel optical approach to atomic force microscopy [*Appl. Phys. Lett.* **53,** 1095 (1988)]: *Appl. Phys. Lett.* **53,** 2400–2402.

Newman, A. C. D. (1987) *Chemistry of Clays and Clay Minerals:* Wiley, New York, 480 pp.

Sposito, G. (1984) *The Surface Chemistry of Soils*: Oxford University Press, New York, 234 pp.

Sposito, G., Holtzclaw, K. M., Johnston, C. T., and LeVesque-Madore, C. S. (1981) Thermodynamics of sodium-copper exchange on Wyoming bentonite: *Soil Sci. Soc. Amer. J.* **45,** 1079–1084.

Sposito, G. and LeVesque, C. S. (1985) Sodium-calcium-magnesium exchange on Silver Hill illite: *Soil Sci. Soc. Amer. J.* **49,** 1153–1159.

Thellier, C. and Sposito, G. (1988) Quaternary cation exchange on Silver Hill illite: *Soil Sci. Soc. Amer. J.* **52,** 979–985.

Theng, B. K. G. (1979) *Formation and Properties of Clay-Polymer Complexes:* Elsevier, Amsterdam, 362 pp.

Weaver, C. D. and Pollard, L. D. (1973) *The Chemistry of Clay Minerals:* Elsevier, Amsterdam, 213 pp.

Wickramasinghe, H. K. (1989) Scanned-probe microscopes: *Sci. Amer.* **260,** 98–105.

(Received 12 January 1990; accepted 2 April 1990; Ms. 1975)

https://doi.org/10.1346/CCMN.1990.0380401 Published online by Cambridge University Press